J|A|C|S ARTICLES

Published on Web 02/01/2010

Phase Diagram of $NdFeAsO_{1-x}F_x$: Essential Role of Chemical Composition

Lorenzo Malavasi,*,† Gianluca A. Artioli,† Clemens Ritter,‡ M. Cristina Mozzati,§ Beatrice Maroni,† Bholanath Pahari,† and Andrea Caneschi||

Dipartimento di Chimica Fisica "M. Rolla", INSTM (UdR Pavia) and IENI-CNR, Università di Pavia, Viale Taramelli 16, 27100 Pavia, Italy, Institute Laue-Langevin, Boite Postale 156, F-38042, Grenoble, France, CNISM, Unità di Pavia and Dipartimento di Fisica "A. Volta", Università di Pavia, Via Bassi 6, I-27100, Pavia, Italy, and Dipartimento di Chimica, and INSTM (UdR Firenze), Università degli Studi di Firenze, I-50019 Sesto Fiorentino (FI), Italy

Received December 15, 2009; E-mail: lorenzo.malavasi@unipv.it

Abstract: In this Article, we provided the complete phase diagram of $NdFeAsO_{1-x}F_x$ solid solution as a function of electron doping thanks to the careful determination of F- and O-content and phase content. We gave direct evidence of the source of F-depletion in the superconducting main phase, that is, the formation of oxyfluoride spurious phase. The approach reported in this work clearly showed that to give reliable results on these complex new superconducting materials, a rigorous control of the chemical composition of the considered phases has to be carried out.

Introduction

The recent discovery of high-temperature superconductivity in *Ln*FeAsO[1] pnictides has triggered the attention of a huge community of solid state physicists and chemists who are working extensively on these new phases to both increase their critical temperature (T_C) and understand their basic mechanism for superconductivity. Soon after the discovery of a T_C of 23 K in the $LaFeAsO_{1-x}F_x$ solid solution, the substitution with other Ln rapidly led to the rise of T_C up to more than 50 K in the $SmFeAsO_{1-x}F_x$ system.[2] The experimental evidence accumulated so far has shown that intriguing couplings between superconductivity and magnetism and structural features are present.[3−6] An essential piece of knowledge to give reliable information on these new systems is the ability to give a clear picture of their phase diagram as a function of F-doping. For $SmFeAsO_{1-x}F_x$, an extensive work was recently published, which addressed this point even though without a magnetic investigation of the studied samples.[7] A complete phase diagram for the $NdFeAsO_{1-x}F_x$ system, which represents one of the most investigated and important members of the pnictide HTSC family, is still lacking in the current literature.

However, apart from these considerations, the experimental works reported until now are, in our opinion, lacking with respect to a fundamental issue, that is, the real chemical composition in terms of F-doping. In pnictide HTSC, the problem with the determination of F-content is not only related to the well-known F volatility at the synthesis temperature currently used (>1000 °C) but also related to the apparently unavoidable formation of lanthanide oxyfluorides phases (*Ln*OF). In the very few papers mentioning these impurities, it was observed that their amount increases with the F-doping, suggesting a progressive increase of F-depletion from the main superconducting phase. We would like to highlight that in all of the papers published on the pnictide HTSC where X-ray or neutron diffraction patterns are shown, there is clear evidence of this phase for F-contents starting from ca. $x = 0.1$ (for a non-exhaustive list of references, see refs 1, 7−9). This behavior can also be related to the progressive reduction of F solubility in the parent *Ln*FeAsO lattice.

In view of these considerations, we are reporting here the phase diagram of the $NdFeAsO_{1-x}F_x$ solid solution where the structural and magnetic properties have been determined on samples of known real F-doping. The structural properties have

† Dipartimento di Chimica Fisica "M. Rolla", INSTM (UdR Pavia) and IENI-CNR, Università di Pavia.
‡ Institute Laue-Langevin.
§ CNISM, Unità di Pavia and Dipartimento di Fisica "A. Volta", Università di Pavia.
|| Università degli Studi di Firenze.

(1) Kamihara, Y.; Watanabe, T.; Hirano, M.; Hosono, H. *J. Am. Chem. Soc.* **2008**, *130*, 3296.
(2) Ren, Z. A.; Lu, W.; Yang, J.; Yi, W.; Shen, X. L.; Li, Z. C.; Che, G. C.; Dong, X. L.; Sun, L. L.; Zhou, F.; Zhao, Z. X. *Chin. Phys. Lett.* **2008**, *25*, 2215.
(3) Marcinkova, A.; Suard, E.; Fitch, A. N.; Margadonna, S.; Bos, J. W. G. *Chem. Mater.* **2009**, *21*, 2967.
(4) Aczel, A. A.; Baggio-Saitovitch, E.; Budko, S. L.; Canfield, P. C.; Carlo, J. P.; Chen, G. F.; Dai, P.; Goko, T.; Hu, W. Z.; Luke, G. M.; Luo, J. L.; Ni, N.; Sanchez-Candela, D. R.; Tafti, F. F.; Wang, N. L.; Williams, T. J.; Yu, W.; Uemura, Y. J. *Phys. Rev. B* **2008**, *78*, 214503.
(5) Drew, A. J.; Niedermayer, Ch.; Baker, P. J.; Pratt, F. L.; Blundell, S. J.; Lancaster, T.; Liu, R. H.; Wu, G.; Chen, X. H.; Watanabe, I.; Malik, V. K.; Dubroka, A.; Rössle, M.; Kim, K. W.; Baines, C.; Bernhard, C. *Nat. Mater.* **2009**, *8*, 310.
(6) Zhao, J.; Huang, Q.; de la Cruz, C.; Li, S. L.; Lynn, J. W.; Chen, Y.; Green, M. A.; Chen, G. F.; Li, G.; Li, Z.; Luo, J. L.; Wang, N. L.; Dai, P. C. *Nat. Mater.* **2008**, *7*, 953.
(7) Margadonna, S.; Takabayashi, Y.; McDonald, M. T.; Brunelli, M.; Wu, G.; Liu, R. H.; Chen, X. H.; Prassides, K. *Phys. Rev. B* **2009**, *79*, 014503.
(8) Chen, X. H.; Wu, T.; Wu, G.; Liu, R. H.; Chen, H.; Fang, D. F. *Nature* **2008**, *453*, 761.
(9) Qiu, Y.; Bao, W.; Huang, Q.; Yildirim, T.; Simmons, J. M.; Green, M. A.; Lynn, J. W.; Kasparovic, Y. C.; Li, J.; Wu, T.; Wu, G.; Chen, X. H. *Phys. Rev. Lett.* **2008**, *101*, 257002.

been determined by means of X-ray diffraction and neutron diffraction. The chemical composition has been determined by a careful electron microprobe analysis (EMPA), while the magnetic characterizations have been carried out by means of a SQUID magnetometer.

Experimental Section

Polycrystalline samples with nominal composition $NdFeAsO_{1-x}F_x$ ($0 \le x \le 0.22$) were synthesized by conventional solid state reactions using high-purity NdAs, SmF_3, Fe, and Fe_2O_3.[10] Each sample batch was about 1 g. NdAs was prepared starting with Nd rods (NewMetals, >99.9%) from which Nd powder was obtained working in glovebox under Ar flux. Pellets of NdAs have been prepared and fired at 500 °C for 2 h and then to 900 °C for 18 h in quartz tubes sealed under vacuum (ca. 10^{-5} bar). The reagents were mixed, pressed in the form of pellets, wrapped in tantalum foils, and left to react at 1160 °C for 48 h in vacuum (ca. 10^{-5} bar)-sealed quartz tubes. The samples were characterized by powder X-ray diffraction and dc magnetization measurements.

For the neutron diffraction measurements, the $NdFeAsO_{1-x}F_x$ ($x = 0$, 0.05, 0.10, 0.15, 0.18, 0.20, and 0.22) samples were sealed in vanadium sample holders and measured at a wavelength of $\lambda = 1.91$ Å at selected temperature points on the high-resolution powder diffractometer D1A at the ILL (Grenoble). Data analysis was performed by Rietveld analysis using the FullProf suite.[11]

The F-content of the measured samples has been determined by means of EMPA. Measurements have been done on selected grains of pure pnictide oxide phase, thus avoiding any interference coming from the neodymium oxyfluoride. To get the best accuracy in the EMPA measurements, great care has been taken in sample preparation, which included the use of sintered pellets that have been polished down to 0.25 μm to achieve planar samples on the micrometer scale. Standards for calibration were selected using materials containing a similar amount of the measured elements as in the pnictide phase with cations and arsenic in the same oxidation state as in the measured samples. Beam acceleration voltage was 15 kV, and beam current was 20 nA. The size of the beam was fixed to 25 μm, and the acquisition time was 10 s on the sample and 5 s on the background. To avoid F-depletion induced by the beam current, we employed a defocused beam, and we checked analytically that no F-loss was present during the EMPA measurements. Finally, the standards used for the calibration were $NdPO_4$ for Nd, Ilmenite A128 for Fe, Fluorite for F, and GaAs for As.

Results and Discussion

Figure 1 shows the correlation between the nominal F-doping (i.e., the stoichiometry of F used in the samples synthesis) against the F-content determined by means of EMPA. As can be appreciated, along with the increase in the F-content, the discrepancy between the nominal and effective F concentration increases. The effective values of F-content are reported in Table 1. As mentioned before, the two possible causes of F-loss are (i) the formation of NdOF and (ii) the evaporation of F during the synthetic procedure.

Figure 2 shows a detail of the neutron patterns collected at room temperature ($\lambda = 1.91$ Å) for the different samples investigated in the present Article. The shown 2θ-range highlights the appearance of the first peak of the NdFO phase (space group R-3c; lattice parameters: $a = b = 3.95786(2)$ Å and $c = 19.70025(7)$ Å)[12] at about $2\theta = 34.5°$. From the Rietveld refinement based on the neutron diffraction data, the

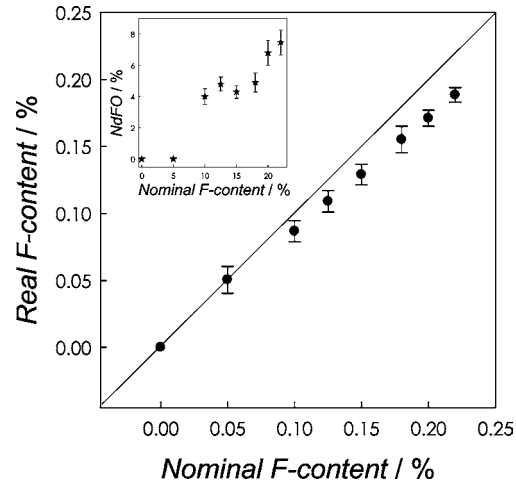

Figure 1. Plot of the nominal F-content of the prepared samples against the real F-content determined by means of EMPA. Inset: Amount of NdOF phase as a function of nominal F-content.

Table 1. Nominal F-Contents, Measured F-Contents, and T_C Values for the $NdFeAsO_{1-x}F_x$ Samples

nominal F	measured F	T_C
0	0	
0.05	0.050(8)	
0.10	0.087(8)	
0.125	0.109(8)	
0.15	0.129(6)	14
0.18	0.155(9)	42.1
0.20	0.171(6)	44.3
0.22	0.188(5)	45

amount of NdOF phase was calculated for each composition. The results are plotted as the inset of Figure 1. A detectable amount of NdFO impurity phase appears at $x = 0.1$ (~4.0(4)%), and its amount increases along with the F-content. The comparison of the two plots of Figure 1 suggests that as soon as the real F-content starts to deviate from the nominal F-content a fraction of F-containing impurity phases forms. The relative amount of missing fluorine is more or less constant for $x \ge 0.1$ and corresponds to about 15% of the initial fluorine content. The calculation of the F-content in the spurious phase accounts

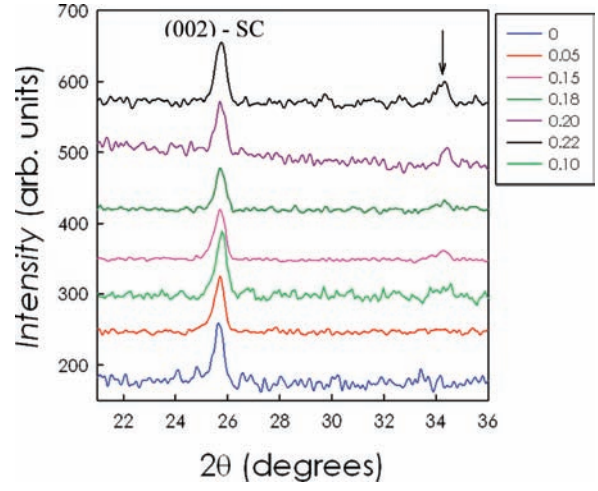

Figure 2. Room-temperature neutron diffraction patterns for the nominal $NdFeAsO_{1-x}F_x$ samples reported in the legend. The first peak refers to the (002) reflection of the pnictide phase (SC, superconductor), while the peak marked with an arrow signs the first peak of the NdOF phase.

(10) Artioli, G. A.; Malavasi, L.; Mozzati, M. C.; Diaz-Fernandez, Y. *J. Am. Chem. Soc.* **2009**, *131*, 12044.
(11) Rodriguez-Carvajal, J. *Physica B* **1993**, *192*, 55.
(12) Beaury, L.; Derouet, J.; Hölsä, J.; Lastusaari, M.; Rodriguez-Carvajal, J. *Solid State Sci.* **2002**, *4*, 1039.

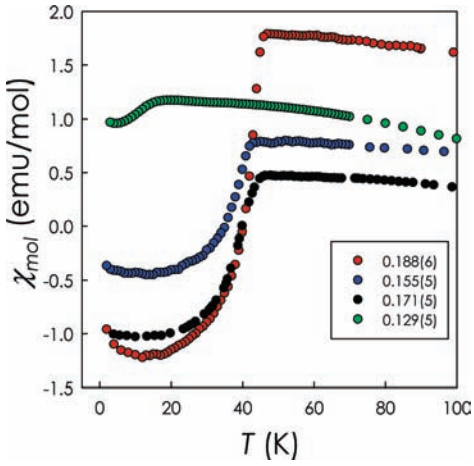

Figure 3. Molar susceptibility curves at 1G for those samples of the $NdFeAsO_{1-x}F_x$ solid solution that show a superconducting transition. F-content values are those determined with the EMPA probe.

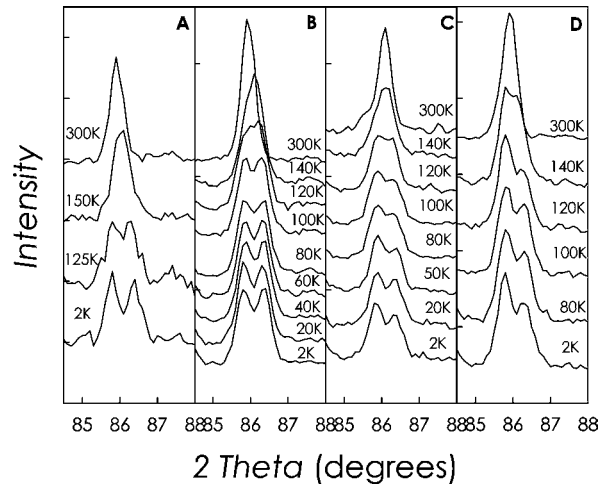

Figure 4. Temperature-dependent neutron diffraction patterns for the nominal $x = 0$ (panel A), $x = 0.05$ (panel B), $x = 0.10$ (panel C), and $x = 0.125$ (panel D) samples of the $NdFeAsO_{1-x}F_x$ solid solution.

for nearly all of the F missed from the main phase, thus suggesting that the critical source of F-depletion in the main phase is not its evaporation during the synthesis but its inclusion in the oxyfluoride phase.

The formation of the NdOF phase may also lead to a reduction of the actual oxygen stoichiometry in the samples, which in turn is a further source of electron doping. To have an insight on this aspect, we have included in the Rietveld refinement the occupancy of the (O,F) site (by considering a "single" site because neutrons cannot distinguish between F and O). Within the estimated standard deviation of the refinements, we could observe a full occupancy (1.0) of this site for all of the samples except for the nominal $x = 0.20$ and 0.22 samples. For the $x = 0.20$ and $x = 0.22$ samples, the complete occupancy of the O,F site was 0.98(1) and 0.97(1), respectively.

To complete the phase diagram of the $NdFeAsO_{1-x}F_x$ solid solution, we collected magnetization data and neutron diffraction data at low temperature. Figure 3 shows the susceptibility curves for the $NdFeAsO_{1-x}F_x$ system relative to those samples that show a superconducting transition. The reported values of the F-content in the legend of the Figure refer now to the real F-content as determined analytically by means of EMPA. The first evidence of a superconducting transition is found for the sample with $x = 0.129(5)$, which shows, however, no bulk superconductivity even with a clear transition around 20 K. Bulk superconductivity is found for $x = 0.155(5)$ with T_C around 40 K, while the maximum value of the transition temperature is ca. 46 K for a real F-concentration of 0.188(6).

To define the tetragonal to orthorhombic phase transition temperature and the presence of magnetic ordering, the structural properties of the prepared samples have been checked as well at low temperature by means of neutron diffraction. Figure 4 shows a selected region of the neutron patterns as a function of temperature for the nominal $F = 0$, 0.05, 0.10, and 0.125 samples. Only for these four samples was it possible to observe a clear splitting of the tetragonal (220) Bragg reflection into the (040) and (400) orthorhombic reflections as already observed in previous systems.[7] Even though the temperature points collected up to now are not very dense, it is clear that all three samples are tetragonal at 140 K and still orthorhombic at 120 K, where a very small splitting between the (040) and (400) reflections can still be seen. This strongly suggests that the temperature for the structural phase transition (T_S) is very close to 120−130 K, but, irrespective to the precise temperature, the interesting fact is that it seems to be only very slightly dependent upon the F-content, contrary to what has been found in the Sm system.[7] Tables reporting the lattice parameter as a function of F-doping at 2 and 300 K are available as Supporting Information.

Concerning the magnetism, for the Nd-systems it is already known that the magnetic ordering of Fe ions occurs around 140 K,[13] while the ordering of Nd ions occurs below 2 K. The Fe magnetic order has been determined in two published neutron powder diffraction studies.[9,13] One finds magnetic ordering below 2 K only, which coincides with the magnetic ordering of the Nd sublattice. The refined moments are $m_x = m = 0.9(1)$ μ_B for Fe and $m_x = 1.22(7)$ μ_B, $m_z = 0.96(9)$ μ_B, and $m = 1.55(4)$ μ_B for Nd.[9] The other demonstrates that the iron moments remain aligned in stripes up to $T_{SDW} = 141(6)$ K ($T_{N,Nd} \approx 2$ K) but with a much reduced moment ($m = 0.25(7)$ μ_B) and a magnetic cell that is doubled along the *c*-axis.[13]

In our present work, we were mainly interested in the structural investigation by means of neutron diffraction (as indicated also by the wavelength choice). In any case, we were able to clearly see magnetic reflections at 2 K due to the Nd-ordering in agreement with the model proposed by Qiu et al.[9] within the *Cmma* crystallographic cell, which are only present for the samples with a nominal F content of 0, 0.05, 0.10, and 0.125, that is, those that also show a structural phase transition and no sign of superconductivity. Fe magnetic peaks have not been observed in our data, most probably due to the statistics, which has been optimized for the nuclear peaks.

A summary of the results presented in this Article is used to construct, in Figure 5, a phase diagram as a function of the electron doping. We were able, for the first time, to provide this kind of diagram by combining the results obtained from the F-content determination and the deficiency on the O,F site determined from the refinement of the site occupancy as explained before. The careful quantitative work realized both on the sample composition and on the amount of impurity phase has shown that the main source of F-depletion in the samples comes from the formation of the Nd oxyfluoride compound.

(13) Chen, Y.; Lynn, J. W.; Li, J.; Li, G.; Chen, G. F.; Luo, J. L.; Wang, N. L.; Dai, P. C.; dela Cruz, C.; Mook, H. A. *Phys. Rev. B* **2008**, *78*, 064515.

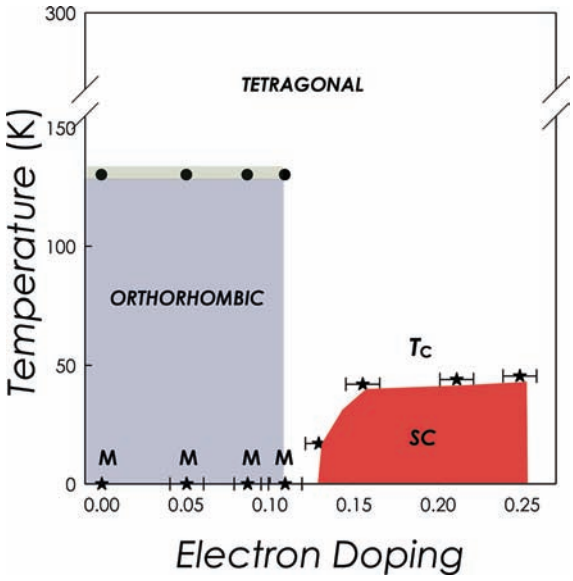

Figure 5. Trend of the transition temperature from the tetragonal to the orthorhombic symmetry (T_S, full circles with gray pattern indicating the uncertainty) and of the critical temperature (T_C, full stars) against the electron doping of the samples. M above the stars in the phase diagram marks those samples that show long-range magnetic ordering at 2 K.

As can be appreciated, the amount of this spurious phase grows significantly as the F-content increases. In addition, evidence of oxygen under-stoichiometry has been found for those samples containing higher amounts of NdOF. This clearly means that all of the data reported up to now in the current literature, where the presence of oxyfluoride phases is evident, should be re-evaluated in view of these results. The claim, for example, of coexistence of superconductivity and magnetism should again be checked in highly controlled samples where, together with oxyfluoride phase, other magnetic impurities, such as Fe, FeAs, may be present. In this case, all of the samples showing a magnetic phase at 2 K are not superconducting, and the magnetic contribution is no more detectable at the first evidence of superconductivity (nominal $x = 0.15$). Some phase diagrams reported in the current literature show an anomalous trend of the critical temperature versus the F-doping at high F-contents such as a plateau-like trend or even a reduction of the T_C.[14] We strongly believe that the reason for these trends has to be searched on the progressive and increasing F depletion from the main phase at high F-contents where, most probably, a solubility limit will be reached.

The results reported here have important implications because they demonstrate that by using a routine method for the preparation of F-doped iron-based HTSCs the obtained final stoichiometry is quite different from the nominal one. The precise definition of the lower limit of F-content for the insurgence of superconductivity and of the T_C versus F trends requires a strict control of F-stoichiometry (and oxygen stoichiometry). It is clear that the role played by F-content in pnictide HTSCs has several similarities to the role played by the oxygen content in cuprate superconductors. In a similar way, after the discovery of HTSC in cuprates, some time was needed before the accurate and precise determination of oxygen content was recognized as the basic issue to provide reliable and comparable results in those materials. This Article just reported the example of F-content determination using electron microprobe analysis, but any other feasible analytical method, with even a higher accuracy, may be of help in this respect (for example, X-ray fluorescence, F^- determination by electroanalytical methods, etc.).

Important issues regarding the chemical control in pnictide HTSC still remain open, among these, the development of routine methods for the exact determination of the oxygen content together with the F-content (because O-deficient samples show superconductivity) and a microscopic investigation of the F-distribution over the sample bulk.

Acknowledgment. Dr. Simona Bigi is gratefully acknowledged for having performed EMPA analysis. The Department of Earth Science of Modena University and CNR of Modena are acknowledged for allowing SEM use. We gratefully acknowledge funding from the CARIPLO Foundation (Project 2009-2540 "Chemical Control and Doping Effects in Pnictide High-temperature Superconductors").

Supporting Information Available: Tables of structural data. This material is available free of charge via the Internet at http://pubs.acs.org.

JA910426D

(14) Sanna, S.; De Renzi, R.; Lamura, G.; Ferdeghini, C.; Palenzona, A.; Putti, M.; Tropeano, M.; Shiroka, T. *Phys. Rev. B* **2009**, *80*, 052503.